
**AIRCRAFT INSTRUMENTS AND
INSTRUMENTATION COMPUTER COMPLEXES**

Numerical Simulation of Air Carrier Radiation Transfer in the Atmosphere

**N. I. Moskalenko^a, R. Sh. Misbakhov^a, I. R. Dodov^{a,*},
M. S. Khamidullina^a, and N. E. Kuvshinov^a**

^a*Kazan State Power Engineering University, ul. Krasnosel'skaya 51, Kazan, 420066 Tatarstan, Russia*

**e-mail: utisey@gmail.com*

Received May 18, 2018; in final form, November 19, 2018

Abstract—The transfer of selective radiation from exhaust flames and traces of air carriers is considered taking into account an acute selection of radiation spectra and radiation absorption spectra by the atmosphere. Numerical simulation of radiation transfer reveals the effects of medium clarification or enhancement of radiation absorption by it, depending on the temperature field and chemical composition of selective radiation sources created by airborne materials in the atmosphere. The effect of the temperature shift of the centers of spectral lines at high temperatures of the air carrier flame on the transfer of their radiation in the atmosphere is noted.

DOI: 10.3103/S1068799819010136

Keywords: radiation transfer, radiative heat exchange, air carriers, equilibrium and non-equilibrium radiation, parameters of spectral lines.

INTRODUCTION

The present work is aimed at the development and application of numerical simulation methods (NSM) for the transfer of selective radiation of air carriers in the atmosphere, taking into account the acute selection of the spectra of radiation sources (exhaust flames and traces of air carriers) and the spectra of radiation absorption by the atmosphere. The main attention is paid to the study of spectral transmission function (STF) as the main characteristic determining the radiative heat transfer in a complex system of “an atmosphere with an integrated selectively radiating medium”. The atmospheric STF for selective radiation sources depends on the composition of emitters and their structural characteristics.

The solution of the problems of the radiation transfer by the NSM requires knowledge of parameters of the spectral absorption lines (SAL) of the optically active ingredients of the radiation sources and the radiation propagation medium and makes it possible to detect the effects of the medium clarification or the enhancement of its absorption of radiation as a function of the temperature field of the radiation sources. As shown in [1–5], for high-temperature radiation sources, the effect of atmospheric clarification is caused by temperature self-reversal of the radiation spectral lines in structurally inhomogeneous media and the displacement of their centers at high temperatures [6].

We note that the effects of acute selection of radiation spectra should be taken into account in media with equilibrium and non-equilibrium sources of radiation. In the presence of a dispersed phase in radiation sources, an optical parameter of the medium, namely, the probability of a quantum survival as an optical characteristic of an inhomogeneous two-phase radiation source has an acute selection.

An array of SAL parameters necessary for carrying out the radiation transfer simulation was prepared taking into account possible applications to high-temperature media. Below, we give a description of use of the SAL parameter arrays.

For the most important component, namely, the water vapor, the arrays of the SAL centers and intensity calculated in [7, 8] were used, taking into account the influence of the interrelation between vibrational and rotational motions and resonance effects. The half-widths of the spectral lines were calculated for temperatures of 200, 300, 800, 1500, 3000 K for collisions of H₂O–N₂ and H₂O–H₂O molecules. For carbon dioxide, an array of 200 000 spectral lines was prepared [7, 9], calculated taking into account the influence of the Coriolis interaction, Fermi resonance, centrifugal affect on the SAL intensity centers. The half-widths of CO₂ lines were taken on the basis of measurement data for the collision of CO₂–CO₂, CO₂–N₂ molecules [9]. For CO, NO, HCl, the SAL parameters were included, which were calculated with consideration of the vibrational-rotational interactions in the vicinity of the main bands and the first overtone. Transitions from the first ten excited vibrational states were taken into account. The intensities (SAL) of CO and NO were calculated in the rigid top approximation [10]. For molecules HCl³⁵, HCl³⁷ and HF, the effect of vibrational-rotational interactions was taken into account in calculating the intensity of the SAL. The dependences of the SAL half-widths on the rotational quantum number for NO, CO, HCl, HF, O₂ were taken from experimental data. In [8, 11], a database was prepared on the SAL parameters for many gas components that make up the atmosphere and combustion products of energy and aviation fuels, which can be used to simulate the transfer of airborne radiation in the atmosphere.

CALCULATION OF THE SPECTRAL TRANSMISSION FUNCTION (STF)

Information on the STF is necessary for solving any problem of radiative transfer and absorption of radiation in the atmosphere. However, the atmospheric STFs for nonselective and selective sources of radiation are significantly different [1, 2, 4, 5, 12]. At the same time, the atmospheric STFs strongly depend on the structural characteristics of the radiation sources and their chemical composition. For nonselective sources of radiation, the atmospheric STFs were well studied and an atlas of the transparency spectra along arbitrarily oriented atmospheric paths was published [3].

For nonselective radiation of the airborne carrier bodies, the one-parameter and two-parameter methods of equivalent mass were developed for STF $\tau_{\Delta\nu}$ calculations in a multicomponent structurally inhomogeneous propagation medium:

$$\tau_{\Delta\nu} = \prod_i \tau_{i\Delta\nu}[L(T)], \quad (1)$$

where i is the number of the gas or aerosol ingredient of the atmosphere; Δ is the spectral resolution; L is the optical path in the medium; T is the temperature. The product in relation (1) is taken for all the ingredients i of the medium. The parametrization of the STF $\tau_{i\Delta\nu}$ is performed by the two-parameter method of equivalent mass, according to which

$$\left(\frac{1}{\ln \tau_{i\Delta\nu}} \right)^2 = \left(\frac{1}{\ln \tau'_{i\Delta\nu}} \right)^2 + \left(\frac{1}{\ln \tau''_{i\Delta\nu}} \right)^2 + \frac{M_i}{(\ln \tau'_{i\Delta\nu})(\ln \tau''_{i\Delta\nu})}, \quad (2)$$

where

$$|\ln \tau'_{i\Delta\nu}| = \int_L k_{iv}[L(T)] \rho_i(L) dL; \quad (3)$$

$$|\ln \tau''_{i\Delta\nu}| = \left\{ \beta_{iv}^{1/m_i}(T) \rho_i[L(T)] P_{ie}^{n_i/m_i}(L) dL \right\}^{m_i}; \quad (4)$$

$$|\ln \tau_{i\Delta\nu}| = \sum_i |\ln \tau'_{i\Delta\nu}[L(T)]|; \quad (5)$$

$$\tau_{\Delta\nu} = \exp \left[- \sum_i |\ln \tau_{i\Delta\nu}[L(T)]| \right]; \quad (6)$$

$$P_{ie}^i(L) = P_{N_2} + \sum_k B_{ik} [L(T)] P_k(L). \quad (7)$$

Here, $\rho_i(L)$ is the concentration of the optically active ingredient i on the optical path L ; $P_{ie}(L)$ is the effective pressure for the optically active ingredient i on the optical path L ; B_{ik} is the factor of broadening of spectral lines for the collisions of the molecules $i-k$; T is the temperature; $\beta_{iv}^{1/m_i}(T)$, m_i , n_i are the parameters of STF $\tau_{i\Delta v}$ in the approximations of weak and strong absorption; M_i is the parameter that determines the transition rate of the STF from the approximation of weak to the approximation of strong absorption. The parameters $k_{iv}(T)$, $\beta_{iv}(T)$, m_i , n_i , M_i , B_{ik} are determined from the data of the experimental studies carried out [3]. For the continual absorption of radiation by the wings of the SAL and the pressure-induced absorption, PIA $m = n = 1$, $M = -1$. For conditions of the blurred rotational structure of the spectrum, $m = 1$, $n = 0$, $M = -1$. For various gas ingredients i , $M_i \in \{0, -1\}$.

In the USSR, for the first time, experimental studies were made of the propagation of radiation from hot gases through the cold gaseous media imitating the atmosphere, and the effects were revealed of enhanced radiation absorption by the atmosphere for low-temperature sources of selective radiation with temperatures $T \leq 1200$ K. Later, the results of these studies were confirmed by numerical simulation in [1, 4]. Creation of high-temperature atlases of SAL parameters of optically active components of the combustion product gas phase and methods for modeling the structural characteristics of the chemical composition of atmospheric emissions from rocket and turbojet engines [12–16] provide the possibility of performing the atmospheric air STF calculations for selective sources of airborne radiation. The STF for a non-uniform atmosphere pressure and temperature can be calculated by the formula

$$\tau_{\Delta v} = \frac{1}{\Delta v} \int_{\Delta} d\nu \tau_{\nu} [P_j(\bar{L}), T(\bar{L}), \bar{L}], \quad (8)$$

where $\tau_{\nu} [P_j(\bar{L}), T(\bar{L}), \bar{L}]$ is the STF for monochromatic radiation:

$$\tau_{\nu} [P_j(\bar{L}), T(\bar{L}), \bar{L}] = \exp \left[- \left\{ \int_{\bar{L}} d\bar{L} \sum_{ij} S_{ij} \int_{\bar{L}} \left\{ T(\bar{L}), b_{ij} [P_j(\bar{L}), T(\bar{L}), \nu_{ij}, \nu] \right\} \rho_j(\bar{L}) \right\} \right]. \quad (9)$$

In formulas (8), (9), ν is the wave number; Δ is the width of the spectral interval; \bar{L} is the geometric path in the medium; T is the temperature; P_j and ρ_j are the partial pressure and concentration of the j th component; S_{ij} , b_{ij} , ν_{ij} are the intensity, contour and center of the i th line of the j th component, respectively. The SAL parameters depend on the temperature, the total pressure and the chemical composition of the radiation propagation medium.

Several modifications of the shape are used for the contour of spectral lines b_{ij} . For the Lorentz form in the gas mixture

$$b_{ij} = \sum_{k=1}^N a_{ijk}(T) P_k / \left((\nu - \nu_{ij})^2 + \left(\sum_{k=1}^N a_{ij}(T) P_k \right)^2 \right), \quad (10)$$

where $a_{ijk}(T)$ is the SAL half-width for the case of a $j-k$ molecule collision. The summation is performed according to the number of components of the gaseous medium N .

It is known that the Lorentz contour for the line is performed only near its center. This fact is confirmed experimentally for CO_2 , CO , N_2O . Therefore, in the calculation programs, a procedure was proposed for calculating the absorption coefficients with an empirical shape of the contour [17–19]:

$$\begin{cases} b_{ij}(\nu) = b_{ij}(\nu) b_{ij}'(\nu); \\ b_{ij}'(\nu) = (\nu - \nu_{ij})^{-\chi_{ij}} \exp[-a_{ij}|\nu - \nu_{ij}| - d_{ij}]^{G_{ij}}, \end{cases} \quad (11)$$

where $\chi_{ij}, a_{ij}, d_{ij}, c_{ij}$ are the experimentally determined parameters.

To calculate the STF at pressures $P < 10000$ Pa, the Voigt contour was used for the line with its analytical approximations and correction (11) for the line wings.

The SAL half-widths for the collisions of $\text{H}_2\text{O}-\text{N}_2$ molecules are calculated by interpolation from the half-width values α_i at fixed temperatures. For other components, the temperature dependence is adopted:

$$\alpha_i(T) = \alpha_i(T_0) \left(\frac{T}{T_0} \right)^{n_1}, \quad (12)$$

where T_0 is the temperature of the initial half-widths $n_1 = 0.5$ (for collisions of radiation-absorbing molecules with $\text{N}_2, \text{O}_2, \text{H}_2$) and $n_1 = 0.7$ (for collisions of optically active molecules $\text{CO}_2-\text{CO}_2, \text{CO}_2-\text{H}_2\text{O}, \text{HCl}-\text{CO}_2$, etc.).

The temperature dependence of the SAL intensities is calculated by the formula

$$S_{ij}(T) = S_{ij}(T_0) \frac{Q_{vj}(T_0) Q_{rj}(T_0)}{Q_{vj}(T) Q_{rj}(T)} \exp \left[\frac{E_{ij}'' (T - T_0)}{kT - T_0 T} \right], \quad (13)$$

where Q_{rj}, Q_{vj} are the rotational and vibrational statistical sums for the j th component; E_{ij}'' is the energy of the lower state, the transition from which the line is provided by; k is the Boltzmann constant. For low temperatures, realized in atmospheres,

$$\frac{Q_{rj}(T_0)}{Q_{rj}(T)} = \left(\frac{T_0}{T} \right)^{n_2}, \quad (14)$$

where $n_2 = 1$ for $\text{CO}_2, \text{NO}_2, \text{CO}, \text{NO}, \text{HCl}, \text{HF}, \text{O}_2$; $n_2 = 1.5$ for $\text{H}_2\text{O}, \text{O}_3, \text{CH}_4, \text{NH}_3, \text{SO}_2, \text{NO}_2$.

The STF for an arbitrary normalized hardware function $\delta(\nu - \nu')$ is determined by the formula

$$\tau_{\delta\nu} = \int_{\delta} d\nu' \tau_{\nu} \delta(\nu - \nu'), \quad (15)$$

where the integration is extended to the region of wave numbers δ , within which the hardware function is different from zero. The hardware function $\delta(\nu - \nu')$ is introduced into the computer in numerical form.

In addition, the calculation program $\tau_{\Delta\nu, \delta\nu}$ provides the possibility of two-dimensional interpolation of the absorption coefficients

$$k_{\nu j} = \sum_{i=1}^{N_j} S_{ij} \left(T(\bar{L}) \right) b_{il} \left[P_j(\bar{L}), T(\bar{L}), \nu_{ij}, \nu \right] \quad (16)$$

depending on the temperature and pressure P_j in the medium. The latter equation allows you to select an integration element $d\bar{L}$ with a smaller partition as compared to the reference values $k_{\nu j}$.

CALCULATION OF THE COEFFICIENTS OF ABSORPTION

Before performing the calculations of the coefficients of absorption (CA), the line intensities are recalculated to the temperature T of interest, and the array of the SAL parameters is filtered to reduce the number of lines and the time for calculating the STF. The filtration is carried out by the ratio in

the line intensities relative to the strongest absorption line in narrow spectral intervals of $\Delta\nu = 5 \div 10 \text{ cm}^{-1}$. The dimension of the array of lines used depends on the temperature and pressure of the gas mixture.

The computation of the STF by the method of direct calculation on a computer is very laborious, especially for inhomogeneous temperatures and pressure traces, so it is important to implement a labor-efficient program for calculating the CA. Before calculating the CA for the j th component, the quantities

$A_{\delta'_k} = \sum_{i=1}^{N_{\delta'_k}} S_{ij} \alpha_{ij}$ and $A_{\delta''_k} = \sum_{i=1}^{N_{\delta''_k}} S_{ij} \alpha_{ij}$ are prepared in sections of width δ' and δ'' . The CA are calculated simultaneously in zones with the width of 50 cm^{-1} .

In the present paper, the following scheme for calculating the CA is realized. The selected point of the spectrum, in which the CA is calculated, is surrounded by the $2\delta'$ neighborhood, within which the contribution of the SAL in the CA is calculated exactly. For all other SALs, their contribution k'_{vj} to k_{vj} is taken into account approximately. At the same time, k'_{vj} in the equally located at $\delta''/2$ points are calculated by the formula:

$$k'_{vj} = \sum_{i=1}^{N_{t'\delta'+t''\delta''}} S_{ij} \alpha_{ij} / D_{ij} + \sum_{i=1}^{N_{\delta'+2t'(k-1)}} A_{\delta'_{ij}} / D_{\delta'_k} + \sum_{i=1}^{N_{\delta''+2t''}} A_{\delta''_{ij}} / D_{\delta''_k}, \quad (17)$$

where $N_{t'\delta'+t''\delta''}$ is the number of lines outside the interval $2\delta''$ surrounded by the neighborhood $t''\delta''$; $N_{\delta'}, N_{\delta''}$ are the numbers of spectral intervals of width δ' and δ'' , respectively, δ'' multiple δ' , $t''\delta''$ multiple δ'' .

$$D_{\delta'_k} = \left(\nu - \nu_{\delta'_k} \right)^2 b'_j \left(\nu - \nu_{\delta'_k} \right), \quad D_{\delta''_k} = \left(\nu - \nu_{\delta''_k} \right)^2 b_j \left(\nu - \nu_{\delta''_k} \right), \\ D_{ij} = \left(\nu - \nu_{ij} \right)^2 b_{ij} \left(\nu - \nu_{ij} \right), \quad (18)$$

where $\nu_{\delta'_k}$ and $\nu_{\delta''_k}$ are the centers of spectral intervals δ'_k , δ''_k . When calculating k'_{vj} at all other points of the spectrum, an interpolation procedure is used.

The NSM of radiation transfer in structurally inhomogeneous media uses integral-differential solutions [1, 2, 4, 5, 7] in STF algorithms, in which the radiation intensities are calculated in a monochromatic approximation and then integrate over the spectrum of the wave number to obtain a solution in integral form. The STF obtained by the NSM of the fine structure of the spectrum can be used to justify approximate methods of calculating the STF and their parametrization. Algorithms for solving the radiation transfer equation are developed for both equilibrium and non-equilibrium radiation processes, for locally thermodynamically equilibrium states of the medium and for nonstationary states, when the structural characteristics of the medium undergo temporary variations. In connection with the enormous amount of calculations in solving the radiation transfer problems in structurally inhomogeneous media with the use of NSM, it is advisable to represent the solutions obtained in the form of "floating libraries" along a grid of varying characteristics (for example, the probability of quantum survival, temperature, pressure), so that when integrating over spectrum of wave numbers to choose ready-made solutions from the base of "floating libraries" by applying interpolation procedures to the grid of ready solutions. The use of such a procedure allows you many times to reduce the expenditure of computer time on the performance of calculations in solving complex radiative heat transfer problems of NSM [1, 2, 5, 7], in meteorology, climatology, power engineering, in predicting strong anthropogenic and environmental impacts on the environment.

EFFECTS OF ACUTE SELECTION OF EMISSION AND ABSORPTION SPECTRA IN STRUCTURALLY INHOMOGENEOUS MEDIA

The manifestation of the effects of acute selection of the emission and absorption spectra, depending on the structure of selective radiation sources and the radiation propagation medium, can vary from

the effects of the enhancement of radiation absorption by the medium to the clarification of the selective radiation propagation medium.

The development of aerospace technology [13], space vehicles and systems for monitoring the earth's atmosphere and underlying surface, forest and man-made fires, energy facilities require studying the effects of radiation selectivity on its transport in structurally nonhomogeneous (heterogeneous) media and the radiation heat exchange. The temperature of combustion products in the combustion chamber of a rocket engine can reach 4500 K, and the temperature of the carrier rocket flame core in the atmosphere is 2500 K [13]. The temperature decreases in the exhaust flame due to the volume expansion at the nozzle exit section. In the exhaust flame, the process of the fuel burn-up can occur, which leads to an increase in the flame temperature as its section is removed from the rocket carrier nozzle exit section (Fig. 1, curves 1–5) to the maximum temperature on its axis. Curves 6, 7 correspond to the flame tail section. Significant differences in the dependences of the STF for homogeneous and inhomogeneous selective radiation emitters τ_s from the STF τ_n for the non-selective radiation are shown in Fig. 2.

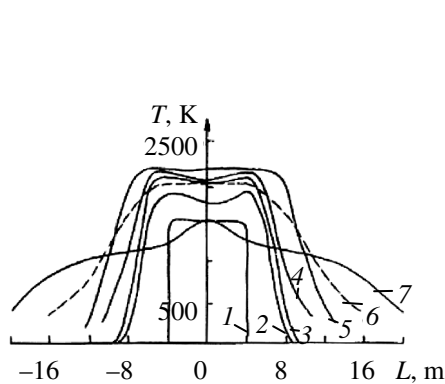


Fig. 1.

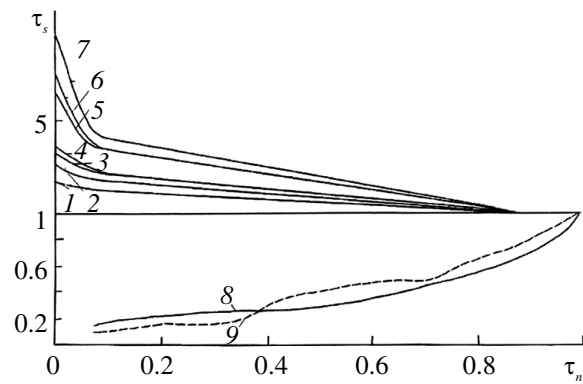


Fig. 2.

Fig. 1. Temperature profiles of emitters 1–7 to the flame sections.

Fig. 2. STF comparison results for selective τ_s and non-selective τ_n radiation from isothermal (curves 8, 9) and nonisothermal (curves 1–7) emitters in the spectral region of 3560–3600 cm^{-1} .

In high-temperature media, it is especially important to select the optimal scheme for calculating the spectral brightness of selective radiation sources. The spatial structure of the emitter is selected in the polar coordinate system, when the rocket carrier axis is set relative to the horizon level, and the temperature field and the ingredient composition of the combustion products are represented as constant temperature isothermal surfaces with a specific grid by volume, which are enclosed in the boundary volume of the selective radiation source. Calculations of monochromatic absorption coefficients are performed on the isothermal surfaces of the radiation source and are represented in the form of a “floating library” in the computer operative memory in the spectral regions $\Delta\nu = 50 \text{ cm}^{-1}$. The spectral brightness of radiation is calculated simultaneously in all directions of observation of the selective emitter, in which the integration elements dL along the optical path L depend on the direction of observation (Fig. 3). In calculating the rate of radiative cooling, the solid angle of the radiation source observation depends on the distance to the radiation source and the zenith and azimuth angles of observation. A geometrical scheme for calculating the spectral brightness of a jet in the atmosphere for various directions of observation is shown in Fig. 3, where TETFIX is the range of observation angles.

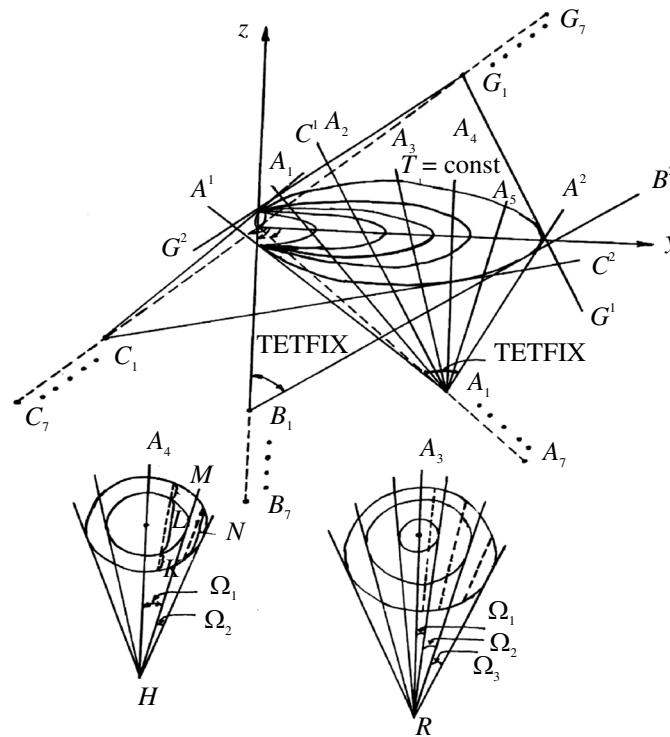


Fig. 3. Geometrical scheme for calculating the spectral brightness of a jet in the atmosphere with different directions of observation (H is the temperature distribution in the section plane that is normal to the flame axis; R is the temperature distribution in the section plane that is inclined to the flame axis).

The z axis is directed along the nozzle exit section, the y axis—is along the axis of the rocket carrier; $C_1 \dots C_7$, $G_1 \dots G_7$, $A_1 \dots A_7$, $B_1 \dots B_7$ are the different directions and distance L to the carrier. A^1-A^2 is the range of zenith angles of scanning; A_1-A_4 is the section perpendicular to the axis of the carrier; A_1-A_3 is the section at an angle to the axis of the carrier.

It can be seen from Fig. 3 that the elementary lengths dL of the path depend on the direction of observation, the zenith and azimuthal angles of scanning of the selective emitter. To calculate the rate of the radiation heating of the atmosphere, it is necessary to calculate the integral radiation flux within the solid angle TETFIX, which depends on the distance L to the nozzle exit section in the atmosphere and on the direction of observation. For radiation detection and observation systems, the detected signal is determined by the field of view of their optical system $\Delta\Omega$. The radiation flux in the atmosphere $F(\Delta\Omega\bar{L})$ can be expressed in terms of the atmospheric STF $\tau_s(\bar{L})$ and the radiation flux $F(\Delta\Omega)$ at the outer edge of the selective radiation source, so that $F(\Delta\Omega\bar{L}) = F(\Delta\Omega)\tau_s(\bar{L})$, where $\tau_s(\bar{L}) = \tau_n(\bar{L})\eta(\bar{L})$, $\eta(\bar{L})$ is the selectivity factor; $\tau_n(\bar{L})$ is the STF for the nonselective radiation source, $\eta(\bar{L}) = \tau_s(\bar{L})/\tau_n(\bar{L})$.

Figures 1, 2, 4 present the results of calculating $\eta(\bar{L})$ for the exhaust flame of a rocket carrier operating on the cryogenic organic fuel (aviation kerosene–oxygen).

The temperature profiles $T(L)$ 1–7 of the emitter (water vapor at $P_{\text{H}_2\text{O}} = 20000$ Pa) correspond to the curves 1–7. The optical thickness of a homogeneous emitter for the experimental 9 and calculated 8 curves is 0.1; $T = 800$ K. The surface layer of the atmosphere has $P_{\text{H}_2\text{O}} = 1000$ Pa. A significant influence

of the selectivity effects on radiative heat exchange and radiation transfer in the atmosphere exposed by strong anthropogenic disturbances follows from the results of studies [1–4]. Earlier, the mechanism of temperature self-reversal of spectral lines, leading to the effect of atmosphere clarification for non-isothermal selective radiation sources, was revealed. In 1987, in “NPO GIPO”, experiments were carried out with registration of radiation transfer for the optically thin selective emitters with a high spectral resolution, which unexpectedly showed the presence of the air clarification effect for a number of spectral ranges of high-temperature water vapor emission (the clarification effect for optically thin emitters according to the mechanism of temperature self-reversal SAL should not be manifested). Only experimental studies of the high-resolution spectra of water vapor [6, 12] revealed the effect of temperature displacement of the centers of spectral lines, which explains the atmosphere clarification for homogeneous selective emitters also, including light molecules (for example, H₂O, CH₄, NH₃ etc.).

Structural characteristics of the selective emitters I–VI (Fig. 4) are presented in Fig. 5.

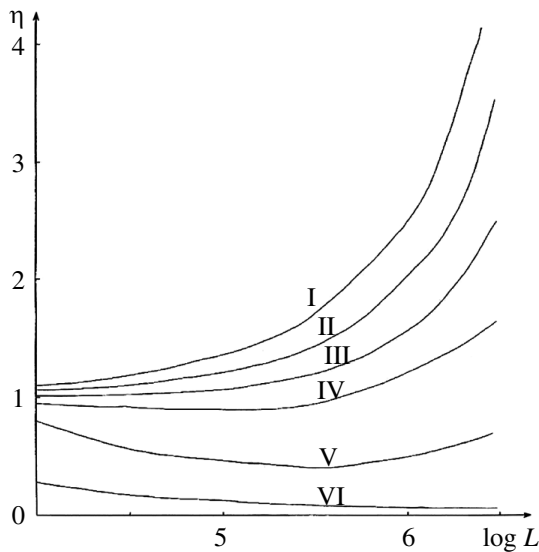


Fig. 4.

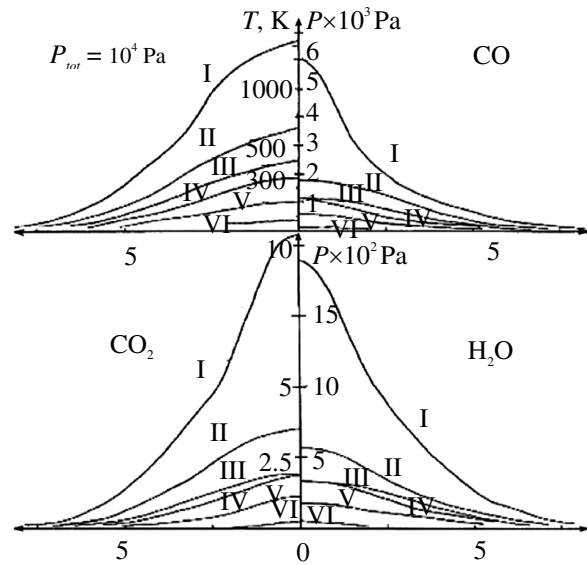


Fig. 5.

Fig. 4. Dependence of the selectivity factor $\eta(\bar{L})$ on the path length in the absorbing atmosphere in the spectral region of 3550–3600 cm^{-1} .

Fig. 5. Structural characteristics of the emitters (I–VI).

CONCLUSIONS

Therefore, we considered the schemes of numerical operational simulation of radiation transfer in solving complex radiative heat transfer problems, including selective radiation sources built into the atmosphere. It was demonstrated that the atmospheric STF for selective radiation sources can differ significantly from the STF for nonselective radiation sources and, depending on the temperature field, can create both intensification of radiation absorption (for temperatures below 1200 K) and the effect of atmospheric clarification for high-temperature inhomogeneous selective emitters (the air carrier exhaust flame, pyrotechnic systems, plasma sources). The data of numerical simulation are confirmed by

the results of laboratory measurements on model atmospheric paths and are explained by the acute selection of emission and absorption spectra of radiation by the atmosphere.

The effect of the intensification of absorption of low-temperature radiation sources by the atmosphere is most intensively manifested for optically thin emitters and significantly affects the radiative heat exchange in conditions of fractional combustion of fuel, enhancing the radiative cooling of the combustion products and heating of the adjacent layers of the atmosphere.

The observed effects of atmospheric clarification for high-temperature selective emitters are provided by the mechanisms of temperature self-reversal and displacement of the centers of spectral lines. Consideration of the acute selectivity of emission spectra in the combustion chambers of power plants leads to an increase in the radiative cooling of high-temperature reaction zones and an increase in the integrated radiation flux on the heat-sensing surfaces of the combustion chamber.

REFERENCES

1. Moskalenko, N.I. and Yakupova, F.S., Solution of Radiation Transfer Problems by Numerical Simulation on a Computer, *Tezisy dokladov 4-go Vsesoyuznogo soveshchaniya po molekulyarnoi spektrometrii vysokogo i sverkhvysokogo razresheniya* (Theses 4th All-Union Meeting on High and Ultrahigh Resolution Molecular Spectrometry), Tomsk: Institut Optiki i Atmosfery, 1978, pp. 178–182.
2. Moskalenko, N.I., Rodionov, L.V., Khamidullina, M.S., and Afanas'ev, I.A. Numerical Modeling of Complex Radiative Heat Transfer, *Izv. Vuz. Problemy Energetiki*, 2015, nos. 1–2, pp. 33–43.
3. Moskalenko, N.I. and Mirumyants, S.O., *Atlas spektrov prozrachnosti po proizvol'no orientirovannym trassam atmosfery* (Atlas of Transparency Spectra of Randomly Oriented Atmosphere Routes), Moscow: TsINII i TEI, 1979.
4. Moskalenko, N.I. and Loktev, N.F., Methods of Modeling the Transfer of Selective Radiation in Structurally Inhomogeneous Media, *Teplovyte Protssesy v Tekhnike*, 2009, vol. 1, no. 10, pp. 432–435.
5. Moskalenko, N.I., Rodionov, L.V., and Yakupova, F.S., Modeling of Radiation Transfer of Flame Pattern of Various Types of Carriers, *Voprosy Spetsial'nogo Mashinostroeniya*, 1984, vol. 2, series 1, pp. 54–58.
6. Moskalenko, N.I., Il'in, Yu.A., and Sadykova, M.S., Investigation of the Emission and Absorption Spectra of Water Vapor, *Izv. Vuz. Fizika*, 2014, vol. 57, no. 9, pp. 3–8 [Russian Physics Journal (Engl. Transl.), 2015, vol. 57, no. 9, pp. 1153–1159].
7. Moskalenko, N.I. and Chesnokov, S.V., Fine Parametrization of Radiation Characteristics of Gas Components of Combustion Products of Hydrocarbon Fuels, *Izv. Vuz. Problemy Energetiki*, 2002, nos. 1–2, pp. 10–19.
8. Rothman, L.S., Gordon, I.E., et al., The HITRAN2012 Molecular Spectroscopic Database, *J. of Quantitative Spectroscopy and Radiative Transfer*, 2013, vol. 130, pp. 4–50.
9. Moskalenko, N.I. and Zotov, O.V., New Experimental Investigations and Refinement of the Spectral Transmission Function of CO₂: Parameters of Lines, *Izv. AN SSSR. Fizika Atmosfery i Okeana*, 1977, vol. 13, no. 5, pp. 488–498.
10. Kayumova, G.V., Moskalenko, N.I., and Parzhin, S.N., Atlas of the Spectral Line Parameters and Absorption of Atmospheric CO, NO, HCl Radiation, *Tezisy dokladov 5-go Vsesoyuznogo simpoziuma po rasprostraneniyu lazernogo izlucheniya v atmosfere* (Theses 5th All-Union Symposium on Propagation of Laser Radiation in the Atmosphere), Tomsk: Institut Optiki i Atmosfery, 1979, vol. 3, pp. 182–186.
11. Alberti, M., Veber, R., Mancini, M., Fateev, A., and Clausen, S., Validation of HITEMP-2010 for Carbon Dioxide and Water Vapor at High Temperatures and Atmospheric Pressures in 450–7600 cm⁻¹ Spectral Range, *J. of Quantitative Spectroscopy and Radiative Transfer*, 2015, vol. 157, pp. 14–33.
12. Alemasov, V.E., et al. *Termodinamicheskie i teplofizicheskie svoystva produktov sgoraniya* (Thermodynamic and Thermophysical Properties of Combustion Products), Glushko, V.P., Ed., Moscow: VINITI, 1972.
13. Alemasov, V.E., Dregalin, A.F., Kryukov, V.G., and Naumov, V.I., *Matematicheskoe modelirovanie vysokotemperaturnykh protsessov v energosilovykh ustanovkakh* (Mathematical Modeling of High-Temperature Processes in Power Plants), Moscow: Nauka, 1989.
14. Tsatiashvili, V.V., Impact of Agents Mixing Velocity in Diffusion Flame on Nitric Oxide Emission, *Izv. Vuz. Av. Tekhnika*, 2013, vol. 56, no. 1, pp. 38–43 [Russian Aeronautics (Engl. Transl.), vol. 56, no. 1, pp. 50–58].

15. Gortyshov, Yu.F., Gureev, V.M., Misbakhov, R.Sh., Gumerov, I.F., and Shaikin, A.P., Influence of Fuel Hydrogen Additives on the Characteristics of a Gas-Piston Engine under Changes of an Ignition Advance Angle, *Izv. Vuz. Av. Tekhnika*, 2009, vol. 52, no. 4, pp. 73–74 [Russian Aeronautics (Engl. Transl.), vol. 52, no. 4, pp. 488–450].
16. Gureev, V.M., Mats, E.B., Ivanova, V.N., Gureev, M.V., Malyshkin, D.A., and Agalakov, Yu.R., Processing Feasibilities of Enhancing the GTE-Based Electric Power Plant Efficiency, *Izv. Vuz. Av. Tekhnika*, 2013, vol. 56, no. 2, pp. 57–60 [Russian Aeronautics (Engl. Transl.), vol. 56, no. 2, pp. 179–184].
17. Moskalenko, N.I., Mirumyants, S.O., Parzhin, S.N., and Dodov, I. R., Measurement System for Study of Absorption Spectra of Gaseous Media at High Pressure, *Zhurnal Prikladnoi Spektroskopii*, 2016, vol. 83, no. 3, pp. 457–461 [J. of Applied Spectroscopy (Engl. Transl.), 2016, vol. 83, no. 3, pp. 449–453].
18. Moskalenko, N.I., Zaripov, A.V., Loktev, N.F., and Il'in, Yu.A., Emission Characteristics of Hydrogen-Oxygen Flames, *Zhurnal Prikladnoi Spektroskopii*, 2010, vol. 77, no. 3, pp. 407–415 [J. of Applied Spectroscopy (Engl. Transl.), vol. 77, no. 3, pp. 378–385].
19. Moskalenko, N.I., Misbakhov, R.Sh., Bagautdinov, I.Z., Loktev, N.F., and Dodov, I. R., Determination of Ingredient Composition of Atmospheric Emissions of the Turbojet Engine Combustion Gases by the Fine-Structure Spectroscopy, *Izv. Vuz. Av. Tekhnika*, 2016, vol. 59, no. 3, pp. 116–124 [Russian Aeronautics (Engl. Transl.), vol. 59, no. 3, pp. 419–425].